

R-09-53

Characterisation of bentonites from Kutch, India and Milos, Greece – some candidate tunnel back-fill materials?

Siv Olsson, Ola Karnland
Clay Technology AB

December 2009

Svensk Kärnbränslehantering AB
Swedish Nuclear Fuel
and Waste Management Co
Box 250, SE-101 24 Stockholm
Phone +46 8 459 84 00



Characterisation of bentonites from Kutch, India and Milos, Greece – some candidate tunnel back-fill materials?

Siv Olsson, Ola Karnland
Clay Technology AB

December 2009

This report concerns a study which was conducted for SKB. The conclusions and viewpoints presented in the report are those of the authors. SKB may draw modified conclusions, based on additional literature sources and/or expert opinions.

A pdf version of this document can be downloaded from www.skb.se.

Abstract

During the past decades comprehensive investigations have been made on bentonite clays in order to find optimal components of the multi-barrier system of repositories for radioactive waste. The present study gives a mineralogical characterisation of some selected bentonites, in order to supply some of the necessary background data on the bentonites for evaluating their potential as tunnel back-fill materials. Two bentonites from the island of Milos, Greece (Milos BF 04 and BF 08), and two bentonites from Kutch, India (Kutch BF 04 and BF 08) were analysed for their grain size distribution, cation exchange properties and chemical composition. The mineralogical composition was determined by X-ray diffraction analysis and evaluated quantitatively by use of the Siroquant software. Both the bulk bentonite and the $<1\ \mu\text{m}$ fraction were analyzed when relevant. Prior to the chemical analyses the $<1\ \mu\text{m}$ fractions were converted to homo-ionic clays and purified by dialysis. The chemical data were used for calculating the structural formula of the smectites. **Milos BF 04** contains ca. 10% particles $>63\ \mu\text{m}$. The bentonite is distinguished by a high content of dolomite and calcite, which make up almost 25% of the bulk sample. The major accessory minerals are K-feldspars and plagioclase, whereas the content of sulphur-bearing minerals is very low (0.06% total S). Smectite makes up around 60% of the bulk sample, which has a CEC value of 73 meq/100 g. The pool of interlayer cations has a composition $\text{Mg}>\text{Ca}>>\text{Na}>>\text{K}$.

The X-ray diffraction characteristics and the high potassium content (1.03% K_2O) of the $<1\ \mu\text{m}$ fraction suggest that the smectite is interstratified with ca. 10% illitic layers. Based on the charge distribution the smectite should be classified as montmorillonite and according to the structural formula, Mg predominates over Fe in the octahedral sheet. However, remnants of Mg-carbonates, if present, may be a source of error in the formula calculation.

Milos BF 08 has a grain-size distribution similar to that of Milos BF 04. The bentonite is low in carbonates but has the highest content of sulphur-bearing minerals (0.99% S) of the bentonites examined. There are strong indications that the major part of sulphur originates from pyrite. Other accessory minerals of significance are Ca-plagioclase (labradorite), kaolin mineral and mica/illite. The bulk sample contains around 70% smectite and has a CEC value of 71 meq/100 g. The pool of interlayer cations has a composition $\text{Ca}>\text{Na}>\text{Mg}>>\text{K}$.

The $<1\ \mu\text{m}$ fraction has a relatively high potassium content (0.43% K_2O) which indicates that also this smectite may be interstratified with a few percent illitic layers. Based on the charge distribution the smectite should be classified as montmorillonite but in this case Fe predominates over Mg in the octahedral sheet. The structural formula suggests that this smectite has the lowest total layer charge of the smectites examined.

Kutch BF 04 contains essentially no particles $>63\ \mu\text{m}$. The bentonite has a high content of titanium- and iron-rich accessory minerals, such as anatase, magnetite, hematite and goethite. Other accessory minerals of significance are feldspars and quartz, whereas the content of sulphur-bearing minerals and carbonates is very low (0.11% S; 0.07% $\text{CO}_3\text{-C}$). The bulk sample contains approximately 80% smectite and has the highest CEC value, 97 meq/100 g, of the bentonites examined. The pool of interlayer cations has a composition $\text{Na}>\text{Ca}>\text{Mg}>>\text{K}$.

The X-ray diffraction characteristics, the very low potassium content (0.04% K_2O) of the $<1\ \mu\text{m}$ fraction and the distribution of the octahedral/tetrahedral charge suggest that the smectite is almost pure montmorillonite. Fe predominates over Mg in its octahedral sheet.

Kutch BF 08 has a similar grain-size distribution as Kutch BF04. Also this bentonite has a very low content of sulphur-bearing minerals and carbonates (0.07% S; 0.02% $\text{CO}_3\text{-C}$) and a high content of Ti- and Fe-rich accessory minerals of the same type as Kutch BF 04 and a similar suite of other accessory minerals. The smectite makes up ca. 80% of the bulk sample, which has a CEC of 89 meq/100 g. The pool of interlayer cations has a composition $\text{Na}>>\text{Ca}=\text{Mg}>>\text{K}$.

The X-ray diffraction characteristics and the very low potassium content (0.02% K_2O) of the $<1\ \mu\text{m}$ fraction suggest that the clay mineral is almost pure smectite but based on the charge distribution this smectite should be classified as beidellite. Fe predominates by far over Mg in its octahedral sheet.

Sammanfattning

Under de senaste decennierna har omfattande undersökningar gjorts på bentonitleror i syfte att hitta optimala barriärmaterial för användning i förvar för utbränt kärnbränsle. Syftet med den nu aktuella undersökningen har varit att ge en mineralogisk karakterisering av några utvalda bentoniter, vilken ska utgöra en del av underlaget för utvärderingen av bentoniternas användbarhet som tunnelåterfyllnadsmaterial.

Två bentoniter från ön Milos, Grekland (Milos BF 04 och Milos BF 08), och två bentoniter från Kutch, Indien (Kutch BF 04 och Kutch BF 08) har analyserats med avseende på kornstorleksfördelning, katjonbytesegenskaper och kemisk sammansättning. Vidare har den mineralogiska sammansättningen bestämts med hjälp av röntgendiffraktionsanalys och utvärderats kvantitativt med hjälp av programvaran Siroquant. Analyserna har gjorts både på totalprov och på fraktionen <math><1\ \mu\text{m}</math>, då så varit relevant. Fraktionen <math><1\ \mu\text{m}</math> mätades med en och samma katjon och renades genom dialys före den kemiska analysen. Kemiska data för fraktionen <math><1\ \mu\text{m}</math> har använts för beräkning av smektitens strukturformel.

Milos BF 04 innehåller c:a 10% grovmaterial >63 μm . Bentoniten har en påfallande hög halt av dolomit och kalcit, som tillsammans utgör nästan 25% av totalprovet. De viktigaste accessoriska mineralen är kaliumfältspat och plagioklas medan innehållet av sulfater och sulfider är mycket lågt (0.06% S). Bulkprovet innehåller ungefär 60% smektit och har ett CEC-värde på 73 meq/100 g. Poolen av utbytbara katjoner har sammansättningen $\text{Mg} > \text{Ca} > \text{Na} > \text{K}$.

Röntgendiffraktionsegenskaperna hos fraktionen <math><1\ \mu\text{m}</math> och dess höga kaliuminnehåll (1.03% K_2O) tyder på att smektiten är blandskiktad med uppemot 10% illit. Utifrån den beräknade fördelningen mellan tetraeder/oktaederladdning ska smektiten klassificeras som montmorillonit. Enligt strukturformeln dominerar magnesium över järn i montmorillonitens oktaederskikt men eventuella rester av Mg-karbonat i <math><1\ \mu\text{m}</math> fraktionen utgör en felkälla i beräkningen.

Milos BF 08 innehåller drygt 10% grovmaterial >63 μm och har således en likartad kornstorleksfördelning som Milos BF 04. Karbonatinnehållet är lågt men bentoniten har den högsta svavelhalten (0.99% S) av samtliga undersökta bentoniter. Mycket tyder på att merparten svavel föreligger som pyrit. Glimmer/illit, Ca-plagioklas (labradorit) och kaolinmineral dominerar bland de accessoriska mineralen. Bulkprovet innehåller ungefär 70% smektit och har ett CEC-värde på 71 meq/100 g. Poolen av utbytbara katjoner har sammansättningen $\text{Ca} > \text{Na} > \text{Mg} > \text{K}$.

Fraktionen <math><1\ \mu\text{m}</math> har ett relativt högt kaliuminnehåll (0.43% K_2O) vilket tyder på att även denna smektit kan vara blandskiktad med ett par procent illit. Enligt den beräknade laddningsfördelningen mellan tetraeder/oktaederskikt ska även denna smektit klassificeras som montmorillonit, men i detta fall dominerar Fe över Mg i montmorillonitens oktaederskikt. Beräkningen tyder också på att montmorillonitens totalladdning är lägre än övriga undersökta smektiter.

Kutch BF 04 innehåller så gott som inget grovmaterial >63 μm . Bentoniten har en väsentligt högre halt av järn, titan och andra tungmetaller än bentoniterna från Milos. Ett flertal titan- och järnrika accessoriska mineral, såsom anatas, magnetit, hematit och goethit, har identifierats med XRD men järn förekommer sannolikt också som röntgenamorfa faser. Andra accessoriska mineral av betydelse är fältspat och kvarts medan halten av svavelförande mineral och karbonater är mycket låg (0.11% S; 0.07% $\text{CO}_3\text{-C}$). Bulkprovet innehåller ungefär 80% smektit och har det högsta CEC-värdet, 97 meq/100 g, av samtliga undersökta bentoniter. Poolen av utbytbara katjoner har sammansättningen $\text{Na} > \text{Ca} > \text{Mg} > \text{K}$.

Röntgendiffraktionsegenskaperna hos fraktionen <math><1\ \mu\text{m}</math>, dess låga kaliuminnehåll (0.04% K_2O) och den beräknade fördelningen mellan tetraeder/oktaederladdning tyder på att lermineralet är en så gott som ren montmorillonit. Järn dominerar över magnesium i smektitens oktaederskikt.

Kutch BF 08 är kornstorleksmässigt likartad Kutch BF04. Även mineralogiskt är de båda indiska bentoniterna likartade – halten av svavelförande mineral och karbonater är mycket låg (0.07% S; 0.02% $\text{CO}_3\text{-C}$) medan Ti- och Fe-rika mineral av samma typ som i Kutch BF 04 är väsentliga

ingredienser bland de accessoriska mineralen, som i övrigt domineras av kvarts och fältspat. Bulkprovet innehåller ungefär 80% smektit och har ett CEC-värde på 89 meq/100 g. Poolen av utbytbara katjoner har sammansättningen $\text{Na} \gg \text{Ca} = \text{Mg} \gg \text{K}$.

Röntgendiffraktionsegenskaperna hos fraktionen $< 1 \mu\text{m}$ och dess låga kaliuminnehåll (0,02% K_2O) tyder på att lermineralet är en mer eller mindre ren smektit, men baserat på den beräknade fördelningen mellan tetraeder/oktaederladdning bör smektiten klassificeras som beidellit snarare än montmorillonit. Järn dominerar stort över magnesium i smektitens oktaederskikt.

Contents

1	Introduction	9
2	Material	11
3	Methods	13
3.1	Sample preparation	13
3.2	Grain-size analyses	13
3.3	Aqueous leachates	13
3.4	Determination of “free iron oxides”	13
3.5	Chemical analysis of the bentonite	14
3.6	Cation exchange capacity (CEC) and exchangeable cations	14
3.7	X-ray diffraction analysis (XRD)	15
3.8	Rietveld analysis of powder diffraction data	15
4	Results	17
4.1	Grain size distribution	17
4.2	Aqueous leachates	17
4.3	CBD-extractable iron	19
4.4	Exchangeable cations and cation exchange capacity	19
4.5	Chemical and mineralogical composition of the bulk bentonites	20
4.6	Chemical and mineralogical composition of the <1 µm fraction of the bentonites	28
5	Summary	34
6	References	35

1 Introduction

During the past decades comprehensive investigations have been made on bentonite clays in order to find optimal components of the multi-barrier system of repositories for radioactive waste. Much of this work has focused on finding suitable bentonite clays for the buffer surrounding the canister, but also on clays that can be used as a component of the tunnel back-fill. The present study presents a mineralogical and chemical characterisation of four bentonites that have been considered such candidate tunnel back-fill materials.

2 Material

Two bentonite samples from Milos, Greece, and two from Kutch, India, have been investigated with respect to their grain size distribution, chemical composition and mineralogy.

The Greek bentonite is quarried in the north-eastern part of the island of Milos, where some of the economically most important bentonite deposits in Europe are concentrated. The island of Milos in the Aegean Sea is part of the Hellenic Arc volcanic province. Pyroclastic tuffs and lavas of andesitic to rhyolitic composition are the main parent rocks of the bentonite, which forms massive bodies having thicknesses of more than 30 m at several sites /Christidis and Dunham 1993/. The two batches of bentonite investigated are referred to as Milos BF 04 and Milos BF 08 in the following text and was delivered by Silver & Baryte Mining Company S.A. in 2004 and 2008, respectively. The Milos bentonite is sold under the name IBECO RWC BF.

The Indian bentonites are from the Kutch area in the Gujarat region in the western part of India. The bentonite is associated with the basaltic Deccan Trap rocks and formed through hydrothermal alteration of volcanic ash in saline water /Shah 1997/. Typically, these bentonites have a dark reddish brown colour imparted by secondary iron oxides. The two batches of bentonite investigated are referred to as Kutch BF 04 and Kutch BF 08 in the following text and were delivered by Ashapura Minechem Co. in 2004 and 2008, respectively.

3 Methods

3.1 Sample preparation

Both the bulk material and the $<1\mu\text{m}$ fraction of the bentonite samples have been analyzed when relevant. The bulk material was not subject to any pre-treatments prior to the analyses, apart from drying at 60°C and grinding.

The fraction $<1\mu\text{m}$ was separated by centrifuged sedimentation. In order to prepare a stable dispersion of the bentonite that allowed a separation of different size fractions, soluble salts were first dissolved by centrifuge-washing with water. The high carbonate content of one of the Milos samples (BF 04) required that carbonates were removed by treatment with an acetic acid-sodium acetate buffer of pH 5 /e.g. Newman and Brown 1987/. This pre-treatment was applied for both Milos samples. After dispersion of the bentonite the suspension was left to rest for 10 minutes to allow sedimentation of the coarsest particles. The supernatant was thereafter collected in centrifuge bottles and centrifuged at 1,550 rounds/min for 5 minutes. The centrifugation time and speed required for sedimentation of particles $>1\mu\text{m}$ was calculated by use of the integrated form of Stokes' Law /e.g Poppe et al. 2001/. After centrifugation the supernatants were collected in plastic containers and concentrated by evaporation at 60°C in a ventilated oven.

3.2 Grain-size analyses

The dried and pre-weighed samples were deflocculated in 0.5% sodium pyrophosphate by ultrasonic treatment and stirring and thereafter wet-sieved through a $63\text{-}\mu\text{m}$ sieve. The $>63\mu\text{m}$ fraction was weighed after drying and its proportion of the bulk was calculated.

The grain size distribution of the fraction $<63\mu\text{m}$ was determined using a Sedigraph Particle analyzer (Micromeritics). The instrument measures the particle size distribution using a finely collimated beam of low energy X-rays, which passes through a container with the suspension to a detector. The change in intensity of the X-ray beam is recorded during the progress of the sedimentation and this X-ray pulse is used to derive the particle size distribution expressed as the mass percent at given particle diameters.

All results have been recalculated to bulk samples.

3.3 Aqueous leachates

Aqueous leaching of the bulk bentonite was used to obtain information about the composition of the soluble salts. The dried and ground bentonite was dispersed in deionised water (solid:solution ratio 1:100) by ultrasonic treatment for 30 minutes and stirring overnight. The suspension was left for 5 days at room temperature to allow equilibration. The supernatant was collected in centrifuge bottles and centrifuged at 3,000 rounds/min for half an hour, and thereafter ultra-filtered through 0.8 and $0.2\mu\text{m}$ syringe filters (Acrodisc PF Syringe Filters) prior to analysis. Major cations were determined by ICP-AES and anions by use of ion chromatography (IC) at the Department of Ecology, Lund University.

3.4 Determination of “free iron oxides”

Iron derived from so called free iron oxides and oxyhydroxides, such as goethite, lepidocrocite, hematite, maghemite, can be extracted more or less selectively using the CBD-method (citrate-bicarbonate-dithionite; /Mehra and Jackson 1960/. The method employs sodium dithionite for the reduction of ferric iron, sodium bicarbonate as a buffer at neutral pH, and sodium citrate as a complexing agent for iron.

The procedure follows the recommendation of /Jackson 1975/. Na-citrate (0.3M) and NaHCO₃ (1M) were added at a ratio of 8:1 to the pre-weighed, dried bentonite sample (1 g) in a centrifuge tube and the temperature of the suspension was brought to 75–80°C in a water-bath. Approximately 0.5 g of Na-dithionite was added by means of a spatula and the mixture was stirred for 5 minutes. The addition of dithionite was repeated twice, or until no reddish coloration of the clay was visible. After centrifugation the supernatant was collected in a volumetric flask. Fe (and Al to estimate the contribution by suspended clay particles) was determined by ICP-AES at the Department of Ecology, Lund University. The CBD-extractable iron content was determined for both bulk samples and <1 µm fractions.

3.5 Chemical analysis of the bentonite

The chemical composition of the bentonites was determined by ICP emission spectrometry (AES) at an ISO 9001 certified laboratory (ACME Analytical Laboratories, Canada), using standard techniques for silicate analysis (fusion with LiBO₂ followed by nitric acid digestion). These analyses include major (Si, Al, Fe, Ca, Mg, K, Na, Mn, P, Ti), and some minor and trace elements (Ba, Co, Ce, Cr, Cu, Nb, Ni, Sc, Sr, Ta, Y, Zn, Zr). Loss on ignition (LOI) was determined as the difference in weight of the dried (at 105° C) and the ignited sample (at 1,000° C).

Total carbon and sulphur were determined by evolved gas analysis (EGA) at the same laboratory by combustion of the samples in a Leco furnace, equipped with IR-detectors for CO₂ and SO₂. Carbonate carbon was determined as CO₂ evolved on treatment of a sub-sample with hot 15% HCl. The distinction of sulphate-S is based on the difference in thermal stability between sulphides and sulphates and was determined for a sub-sample that had been pre-ignited at 800° C.

The purified clay fraction (<1 µm) was converted to homo-ionic Na-clay and Sr-clay, respectively, by addition of NaCl or SrCl₂ solutions (analytical grade reagents) to a final concentration of 1M/0.5M. After flocculation of the clay the clear supernatant was removed and the salting-out cycle was repeated once. Excess salts were removed by centrifuge-washing with water. The Na-clays could be washed only twice since the dispersed clay no longer settled at lower salt concentration. The washing step was followed by dialysis (Spectrapore 3, 3500 MWCO dialysis membrane) against deionised water until the electrical conductivity of the external solution remained <10 µS/cm for five days. The purpose of saturating the exchange sites with one single cation is to make the allocation of cations to exchange and structural sites, respectively, less ambiguous.

All samples were ground, dried at 105°C and stored in desiccators prior to the chemical analysis, i.e. all analytical results are expressed in wt% (major oxides) or ppm (trace elements) of the dry mass of the sample.

3.6 Cation exchange capacity (CEC) and exchangeable cations

The cation exchange capacity (CEC) of bulk materials and of clay fractions (<1 µm) was determined by exchange with copper(II)triethylenetetramine following the procedure of /Meier and Kahr 1999/, modified according to /Ammann et al. 2005/ to ensure complete exchange. The ground sample (400 mg) was dispersed in 50 ml deionised water by ultrasonic treatment. 20 ml of 15 mM Cu(II)-triethylenetetramine solution was added to the suspension, which was left to react for 30 minutes on a vibrating table. After centrifugation the absorbance at 620 nm of the supernatant was measured using a spectrophotometer (Shimadzu). CEC was calculated on the basis of the uptake of Cu by the clay. The water content of the clay was determined for a separate sample dried at 105° C to a constant weight. All CEC determinations were at least duplicated.

The exchangeable cations of the bulk bentonite were also extracted into alcoholic ammonium chloride solution (0.15M NH₄Cl in 80% ethanol) according to a procedure originally recommended for CEC determinations of gypsiferous/calcareous soils /e.g. Belyayeva 1967, Jackson 1975/. An alcoholic solution is used to minimize dissolution of gypsum and calcite, which are soluble or relatively soluble in aqueous solutions. Ideally, i.e. when there are no easily soluble salts such as chlorides and carbonates of alkali metals present, the sum of cations extracted should be equivalent to the CEC of the sample.

0.8 g of the ground sample was shaken for 30 minutes in approximately one third of a total volume of 50 ml of the extractant. After centrifugation the supernatant was collected in a volumetric flask. This treatment was repeated twice. After evaporation of the alcohol and dilution with deionised water, the concentration of Ca, Mg, Na and K in the extracts was determined by use of an ICP-AES equipment at the Department of Ecology, Lund University. The water content of the bentonite was determined for a separate sample. All determinations were duplicated.

3.7 X-ray diffraction analysis (XRD)

The mineralogical composition was determined by X-ray diffraction analysis of two different types of preparations, one type consisting of unsorted and randomly oriented powders of the bulk materials, the other type consisting of aggregates with maximised preferred orientation of the clay minerals.

The random powder of the bulk sample produces "three-dimensional fingerprints" of all minerals and are needed for a general characterization of the materials. Also the distinction between di- and trioctahedral types of clay minerals by measurements of $d(060)$ requires an X-ray diffraction profile of a randomly oriented sample.

The bulk material was ground in an agate mortar to a grain-size $<10 \mu\text{m}$. Since the basal spacing of smectites varies not only with the type of interlayer cations but also with the hydration state of the cations, the samples were equilibrated in desiccators at a relative humidity of ca. 55% during a minimum of 5 days. X-ray scans were made as soon as possible after removal of the samples from the desiccators, but there was no RH control of the goniometer chamber during the scanning. The random powders were scanned with a step size of $0,02^\circ 2\theta$ in the 2θ interval $2-66^\circ$ with a scanning speed of $1^\circ 2\theta/\text{min}$.

The oriented specimen of the fine clay fraction gives strongly enhanced basal ($00l$) reflections, and little or no evidence of the hk reflections of clay minerals. This type of preparation is useful for identification of the clay minerals and of interstratified structures and is also used for tests of the swelling properties of the clay after the clay has been solvated with a polyalcohol, such as ethylene glycol. However, the diffraction characteristics of smectites both in the air-dried and the ethylene glycol solvated state depend on the type of interlayer cations. Therefore, in order to give unambiguous diffraction characteristics, all clay samples were saturated with one single cation (Mg) prior to the X-ray scanning.

The $<1\mu\text{m}$ fractions were deflocculated in deionised water, saturated with Mg added as MgCl_2 to a final concentration of 0.5 M and excess salt was thereafter reduced as much as possible by repeated centrifuge-washing. Oriented aggregates were prepared of the clay slurry according to the "smear-on-glass" method" /Moore and Reynolds 1989/ and dried at room temperature. The oriented mounts were X-ray scanned with a step size of $0,02^\circ 2\theta$ in the 2θ interval $2-36^\circ$ with a scanning speed of $1^\circ 2\theta/\text{min}$. In order to test the swelling properties the samples were re-scanned after solvation with ethylene glycol (EG) at 60°C for 48 hours.

A Seifert 3000 TT X-ray diffractometer with $\text{CuK}\alpha$ radiation and automatic slits was used for the X-ray diffraction analyses.

3.8 Rietveld analysis of powder diffraction data

The mineralogical composition of the bulk samples was evaluated quantitatively from the X-ray diffractograms (Figure 4-2 to 4-5) by use of the Siroquant quantitative XRD software. The modelling is based on the Rietveld refinement method of least squares fit of calculated and measured XRD profiles /Rietveld 1969/. The method is described in /Tailor and Matulis 1994/. The analyses were made in a standardised way, which included a first step of mineral identification based on peak positions and a subsequent quantitative modelling by use of the Siroquant mineral database until no major improvement in pattern fit was achieved.

4 Results

4.1 Grain size distribution

The grain-size distribution of the samples is shown in Figure 4-1.

Both samples from Milos contain more coarse material than the Indian bentonites. Between themselves the Milos samples have similar grain-size distributions, both containing approximately 10% particles >63 μm and 65–70% particles <1 μm . It is uncertain, though, whether dispersion of Milos BF 04 is complete since the high carbonate content of this sample most likely affects the dispersion unfavourably.

Also the two Kutch samples have similar grain-size distributions containing approximately 85% particles <1 μm and essentially no particles coarser than 63 μm . However, the coarse particles are probably somewhat underestimated because magnetic and/or heavy mineral particles (e.g. magnetite, anatase) will escape analysis by sedimentation, when performed in an aqueous medium using a magnetic stirrer to keep the sample in suspension.

4.2 Aqueous leachates

The chemical data on non-reactive solutes and “water-soluble salts” of the bulk bentonites are given in Table 4-1. The samples from Kutch contain considerably more chloride than the Milos samples. Milos BF 04 has the lowest content of soluble sulphur compounds, whereas the sulphate content is in the same range, 1–1.3 mg S/g dry matter, in Milos BF 08, Kutch BF04 and Kutch BF08.

Focus is laid on the major anions since the concentration of the cations is strongly affected by exchange reactions that take place when divalent cations are released from dissolving minerals during the contact with water. Moreover, the sources of some of the cations included in the analysis, such as Al, Fe, Si, are most likely ultra-fine mineral particles which the filtering method failed to remove from the solution.

Table 4-1. Major anions and cations (mg/g dry clay) extracted by dispersion of bentonite in deionised water in a solid:liquid ratio of 1:100. n.d. = not determined. DOC=dissolved organic carbon, IC=inorganic carbon, DN=dissolved nitrogen.

Sample id	Al mg/g dry clay	Ca	Fe	K	Mg	Na	S	Si	Cl	SO ₄ -S	DOC	IC	DN
Milos BF04	0.035	0.36	0.03	0.35	0.17	1.48	0.1	0.361	0.12	0.10	0.14	0.97	0.02
Milos BF08	0.086	0.22	0.035	0.19	0.08	3.25	1.46	0.95	0.1	1.02	n.d.	n.d.	n.d.
Kutch BF04	0.334	0.11	0.29	0.09	0.09	7.13	1.22	1.147	3.56	1.30	1.76	0.56	0.08
Kutch BF08	1.09	0.11	1.1	0.07	0.21	4.67	0.95	3.879	3.7	1.04	2.03	0.05	0.07

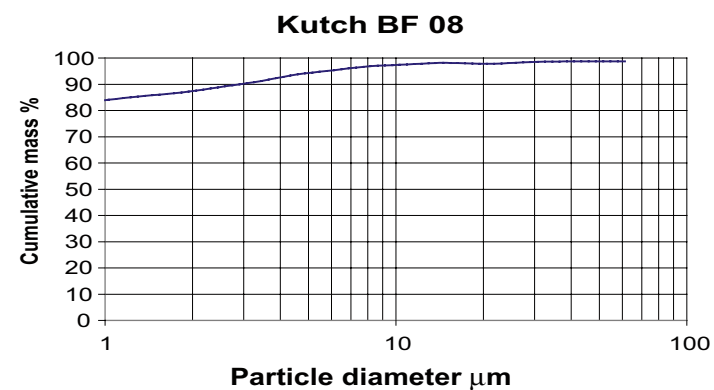
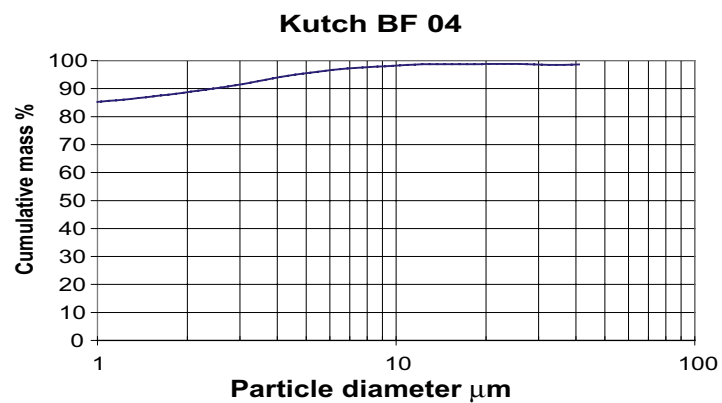
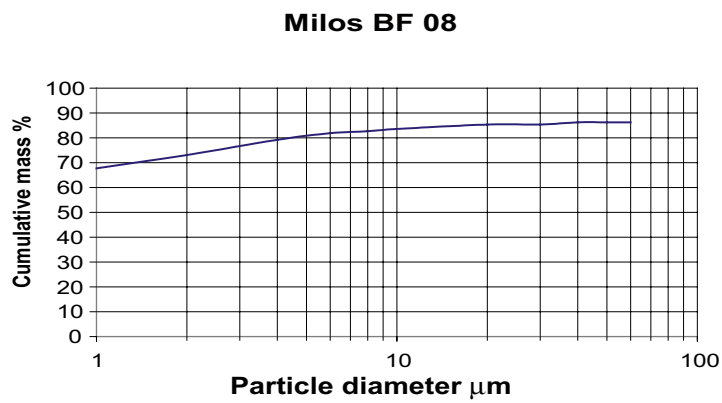
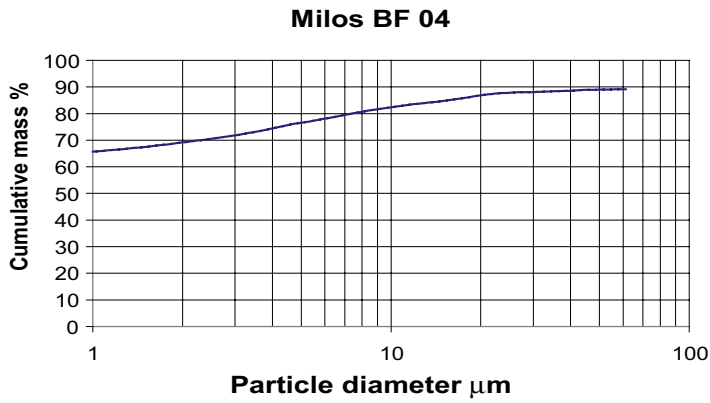


Figure 4-1. Grain-size distribution of the bentonites Milos BF 04, Milos BF 08, Kutch BF 04 and Kutch BF 08.

4.3 CBD-extractable iron

The CBD-extractable iron content of the bulk samples is listed in Table 4-2. The two Indian bentonites are iron-rich (total iron 13.4 and 16.2% Fe₂O₃) and have a dark reddish brown colour imparted by secondary iron oxides/oxyhydroxides. 24–29% of their total iron content (as Fe₂O₃) is extractable by the CBD-method.

In contrast, the yellowish or greenish samples from Milos have much lower total iron content (5.3 and 6.4% Fe₂O₃) and a minor fraction (2–6%) of it is extracted into the CBD-solution.

4.4 Exchangeable cations and cation exchange capacity

The data on the pool of cations extracted by exchange with ammonium in alcoholic solutions are summarised in Table 4-3. The cation pool of the sample Milos BF04 is Mg-Ca dominated, which is in harmony with the high content of Mg/Ca carbonate of the sample (cf. XRD-data below). Calcium is the predominant exchangeable cation also in Milos BF 08, but the proportion of sodium exceeds that of magnesium. Potassium is a minor component of the cation pool in all samples but the Milos bentonites have significantly higher concentrations of exchangeable potassium than the Kutch bentonites.

Table 4-2. CBD-extractable iron and aluminium expressed as oxides in weight % of the dry matter. Total iron and aluminium concentrations of the bentonites (from Table 4-5) are also given together with the CBD-extractable fractions.

Sample id	CBD-extractable		Total		Fraction CBD-extractable	
	Al ₂ O ₃ %	Fe ₂ O ₃ %	Al ₂ O ₃ %	Fe ₂ O ₃ %	Al ₂ O ₃	Fe ₂ O ₃
Kutch BF04	0.101	3.96	14.90	16.17	0.007	0.24
Kutch BF08	0.119	3.95	17.53	13.41	0.007	0.29
Milos BF04	0.065	0.33	13.63	5.27	0.005	0.06
Milos BF08	0.033	0.15	18.60	6.40	0.002	0.02

Table 4-3. Exchangeable cations of duplicate samples of Milos BF 04, Milos BF 08, Kutch BF 04 and Kutch BF 08. Cations extracted by exchange with NH₄⁺ in alcoholic solut

Sample id	Ca		K		Mg		Na		Sum
	meq/100 g	%	meq/100 g	%	meq/100 g	%	meq/100 g	%	
Milos BF 04-1	29	40	2.4	3.3	34	47	7	10	72
Milos BF 04-2	29	41	1.5	2.1	35	49	6	8	72
Milos BF 08-1	31	44	1.6	2.2	17	24	21	30	70
Milos BF 08-2	29	43	1.4	2.1	16	24	20	31	66
Kutch BF04-1	34	31	0.5	0.5	15	13	61	56	110
Kutch BF04-2	33	31	0.5	0.4	14	14	58	55	105
Kutch BF08-1	11	9	0.5	0.5	13	11	89	79	113
Kutch BF08-2	12	9	0.4	0.3	13	10	105	81	130

The exchangeable cation pool of both samples from Kutch is Na-dominated (ca. 55 and 80% Na, respectively). Ca is the second most abundant exchangeable cation (31%) in Kutch BF 04, whereas Ca and Mg make up equal proportions (ca. 10%) of the cation pool of Kutch BF 08. The sum of cations is generally higher than the CEC of the sample (cf. Table 4-3 and Table 4-4) and values for sodium, in particular, varies between duplicate samples. This fact reflects the problems inherent with extraction methods for exchangeable cations: non-reactive solutes and easily soluble salts, such as chlorides and carbonates of alkali metals, will necessarily contribute to the extractable cation pool. The data on the water extracts for the two Kutch samples (Table 4-1) suggest that these samples contain approximately 10 meq Cl⁻/100 g dry sample. Consequently, at least 10 meq of the cations extracted into the ammonium solution may be derived from chlorides.

The data on the cation exchange capacity (Cu-CEC) of the bulk samples are compiled in Table 4-4. The CEC values of the two samples from Milos are in the same range, 71–73 meq/100 g, and significantly lower than the CEC of the Kutch samples (89 and 97 meq/100 g, respectively).

4.5 Chemical and mineralogical composition of the bulk bentonites

The chemical composition of the bulk samples is given in Table 4-5. The XRD-profiles of random powders of the bulk samples are shown in Figure 4-2 to 4-5. Tables 4-6 to 4-9 present the results of the quantitative evaluation of the mineralogy by use of the Siroquant software, together with the resulting chemical composition. The normative calculation of the accessory minerals is based on their ideal formulas, e.g. KAlSi₃O₈ for K-feldspars and Al₂Si₂O₅(OH)₄ for kaolin minerals. The normative calculation of the smectite of individual samples is based on the chemical composition of the <1 μm fraction (Table 4-10) together with the proportional composition of the exchangeable cation pool (Table 4-3). A comparison of the calculated and determined chemical composition gives some idea about the accuracy of the quantitative evaluation of the XRD data and/or of the normative calculations of the minerals identified. In the tables the smectite is listed as montmorillonite. Strictly, the smectite of Kutch BF 08 should be classified as beidellite based on its charge distribution (cf. Table 4-12) but beidellite cannot be distinguished from montmorillonite by the routine XRD-examination used.

In the XRD-traces the strongest peaks of the major non-phyllsilicates, such as quartz, K-feldspar, plagioclase, calcite, dolomite, anatase, various iron oxides, are indicated when relevant. Also the first order basal reflection and the two-dimensional hk-bands of smectite are indicated in the traces. Special attention is paid to the position of the hk-peak (060), which is useful for recognizing di- and trioctahedral sub-groups of clay minerals.

This peak includes the *b* cell dimension which is more sensitive to the size of the cations and to site occupancy in the octahedral sheet than are the *a* or *c* cell dimensions. For smectites the (060)-peak is distinct enough to allow an estimate of the *b* parameter to an accuracy of approximately ±0.5% / Brindley and Brown 1980/.

Table 4-4. Cation exchange capacity (CEC) in milliequivalents per 100 g dry bulk bentonite Milos BF 04, Milos BF 08, Kutch BF 04 and Kutch BF 08. CEC determined for triplicate samples by exchange with the Cu-triethylene tetramine complex.

Sample id.	CEC-1	CEC-2	CEC-3	CEC-mean
	meq/100 g			
Milos BF 04	74	73	73	73
Milos BF 08	72	69	73	71
Kutch BF04	97	98	96	97
Kutch BF 08	89	89	90	89

Table 4-5. Chemical composition of the bulk bentonite samples Milos BF 04, Milos BF 08, Kutch BF 04 and Kutch BF 08. Major, minor and trace elements determined by IPC-AES, S and C by evolved gas analysis in a Leco furnace. n.d. = not determined.

Sample id.	SiO ₂ %	Al ₂ O ₃ %	Fe ₂ O ₃ %	MgO %	CaO %	Na ₂ O %	K ₂ O %	TiO ₂ %	P ₂ O ₅ %	MnO %	Cr ₂ O ₃ %	LOI %	Sum %	Tot C %	Tot S %	CO ₂ -C %	SO ₄ -S %
Milos BF 04	40.93	13.63	5.27	7.60	11.41	0.27	1.11	0.6	0.16	0.2	0.013	18.7	100.0	3.39	0.06	3.01	0.03
Milos BF 08	58.35	18.6	6.40	2.57	2.10	1.13	0.49	0.74	0.21	0.02	<0.002	9.2	99.9	0.16	0.99	0.14	0.17
Kutch BF 04	51.05	14.90	16.17	3.26	1.98	1.87	0.06	2.94	0.29	0.2	0.013	7.2	100.1	0.21	0.11	0.07	0.11
Kutch BF 08	51.93	17.53	13.41	2.35	0.98	2.61	0.08	3.43	0.43	0.07	0.015	7.1	100.1	0.18	0.07	0.02	0.04

Table 4-5 continued.

Sample id.	Ba ppm	Cu ppm	Zn ppm	Ni ppm	Co ppm	Sr Ppm	Zr ppm	Ce ppm	Y ppm	Nb ppm	Sc ppm	Ta ppm
Milos BF 04	564	22	65	36	11	165	116	31	14	12	12	<5
Milos BF 08	968	19	81	<20	n.d	151	196	n.d	20	16	14	n.d
Kutch BF 04	13	268	147	78	73	131	158	26	29	22	41	11
Kutch BF 08	<5	234	125	89	61	76	187	30	43	28	46	<5

Milos BF 04 and Milos BF 08

Milos BF 04 is low in sulphur-bearing minerals but is distinguished by a very high content of carbonates (3.01% acid-soluble C), parallel with high concentrations of CaO and MgO. Thus, the chemical data suggest that the carbonate fraction consists of both Ca and Mg carbonates, which is confirmed by the XRD analysis showing that dolomite ($\text{CaMg}(\text{CO}_3)_2$) and calcite (CaCO_3) are significant constituents of the sample (Figure 4-2). Stoichiometrically the concentration of acid-soluble C alone corresponds to 15% CO_3^{2-} and the quantitative evaluation of the XRD data suggests that dolomite plus calcite make up almost 25% of the sample (Table 4-6).

In contrast, Milos BF 08 has a low carbonate content (1.3% CaCO_3 if all C is allocated to a Ca-carbonate phase) but the highest total sulphur content (0.99% S) among the bentonites investigated. The determination of sulphate-S by use of a Leco furnace (i.e. the distinction of sulphates is based on the difference in thermal stability between sulphides and sulphates) suggests that the major fraction of sulphur, ca. 0.8% S, is derived from sulphides. Similarly, the composition of the aqueous leachate (Table 4-1) indicates that soluble sulphur compounds contribute 0.1–0.15% S, suggesting that the remnant fraction of S is derived from sulphides and/or sparingly soluble sulphates (e.g. barite). If all the remnant sulphur is allocated to pyrite it corresponds to around 1.5% FeS_2 . The quantitative evaluation of the XRD-data gives a similar pyrite concentration and barite cannot be detected in the XRD-trace (Figure 4-3 and Table 4-7).

Both Milos bentonites have considerably higher potassium content (1.11 and 0.49% K_2O) than the bentonites from Kutch (0.06–0.08% K_2O). K-bearing minerals common in bentonites are potassium feldspars (mainly orthoclase and/or sanidine), mica/illite, and mixed layered illite/smectite (and sometimes zeolites). Peaks of K-feldspar (KAlSi_3O_8) are clearly seen in the XRD-trace of Milos BF 04, whereas discrete micaceous minerals, which have their (001) reflection at 10 Å, can barely be detected in this sample. However, the analysis of the $<1\mu\text{m}$ fraction indicates that some of the K-bearing minerals are very fine-grained and probably exist as illitic layers in the structure of the smectite (I/S; cf. para. 4.7). Therefore, a correction has been made for I/S in the Siroquant results obtained for the bulk bentonite in Table 4-6.

In Milos BF 08 mica/illite seems to be a major source of potassium, but also in this case the analyses of the $<1\mu\text{m}$ fraction indicate that some potassium is derived from illite/smectite mixed layers. The predominant feldspar in Milos BF 08 is a Ca-rich plagioclase. The best fit between the peak positions/peak intensities of calculated and measured XRD profiles was obtained for labradorite, which has compositions ranging from $\text{Ab}_{30}\text{An}_{70}$ to $\text{Ab}_{50}\text{An}_{50}$. After allocation of CaO to calcite, gypsum and interlayers, the remnant CaO concentration corresponds to a composition of approximately $\text{Ab}_{30}\text{An}_{70}$ which has been used in the normative mineral calculation given in Table 4-7.

According to the quantitative modelling Milos BF 04 has somewhat lower smectite content (ca. 60%) than Milos BF 08 (ca. 70%) and yet, the two bentonites have similar CEC-values, which suggests a difference between the smectites in their total layer charge (cf. para 4.7). The smectite of both samples produces a fairly well-defined first order basal reflection at 14.7–14.9 Å. The basal spacing is consistent with the pool of interlayer cations, which consists predominantly of divalent cations (cf. Table 4-3). With divalent interlayer cations, the two layer hydrate (basal spacing around 15 Å) predominates over an extensive range of relative humidities /eg. Brindley and Brown 1980/.

Milos BF 04 bulk

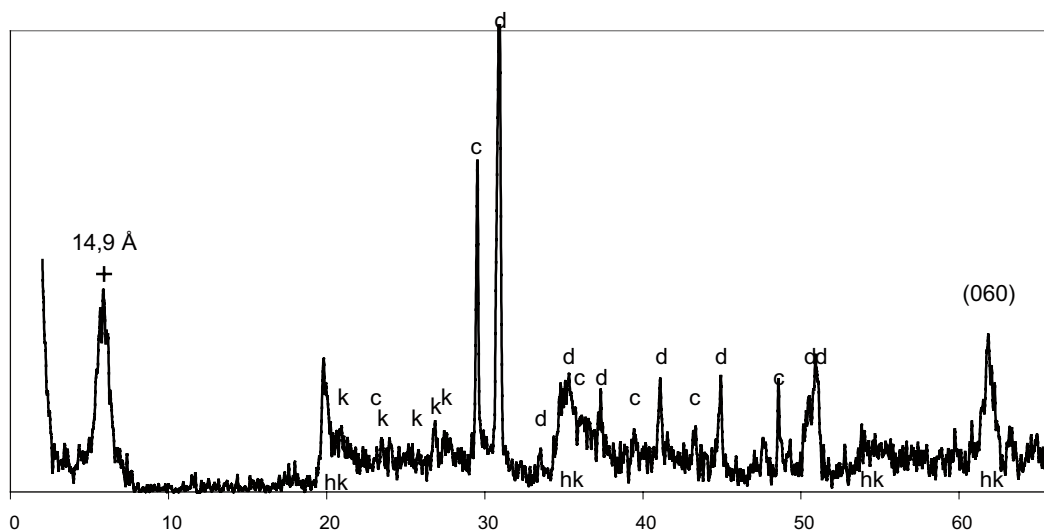


Figure 4-2. XRD-profile of random powder of the bulk sample Milos BF 04. The position of the strongest peaks of the major non-clay minerals is indicated; c=calcite, d=dolomite, k=K-feldspar. The (001) peak of Ca (Mg)-smectite at 14.9Å, the positions of the hk-bands and the (060)-peak are also indicated. CuKα radiation.

Table 4-6. Quantitative evaluation of the XRD data for the bulk of Milos BF 04 by use of the Siroquant software. The resulting chemical composition is given together with the results of the chemical analysis of the sample (ICP-AES and evolved-gas analysis) for comparison.

Siroquant Mineral phases	Normative mineral composition												
	%	Si %	Al %	Ti %	Fe %	Mg %	Ca %	Na %	K %	P %	C %	S %	
Montmorillonite	58	16.71	6.05	0.44	2.36	1.6	0.49	0.12					
Mixed layer illite	6	1.44	0.72	0.04	0.23	0.12			0.43				
Calcite 1	8						3.22				0.97		
Dolomite	16					2.13	3.51				2.1		
Gypsum	0.8						0.2					0.16	
Hematite	1.3				0.94								
Labradorite	1.4	0.37	0.21				0.1	0.06					
Magnetite	1.7				1.22								
Microcline	1.7	0.52	0.17						0.24				
Orthoclase 1	4	1.30	0.41						0.60				
Σ	100	20.34	7.56	0.48	4.75	3.85	7.52	0.18	1.27	0.00	3.07	0.16	
Oxides		SiO ₂	Al ₂ O ₃	TiO ₂	Fe ₂ O ₃	MgO	CaO	Na ₂ O	K ₂ O	P ₂ O ₅	CO ₂ -C	Tot S	Σ excl O/H
Σ		43.6	14.3	0.8	6.8	6.4	10.5	0.2	1.5	0.0	3.1	0.16	87.4
ICP-AES													
Milos BF 04		40.9	13.6	0.6	5.3	7.6	11.4	0.3	1.1	0.2	3.0	0.06	84.1

Milos BF08 bulk

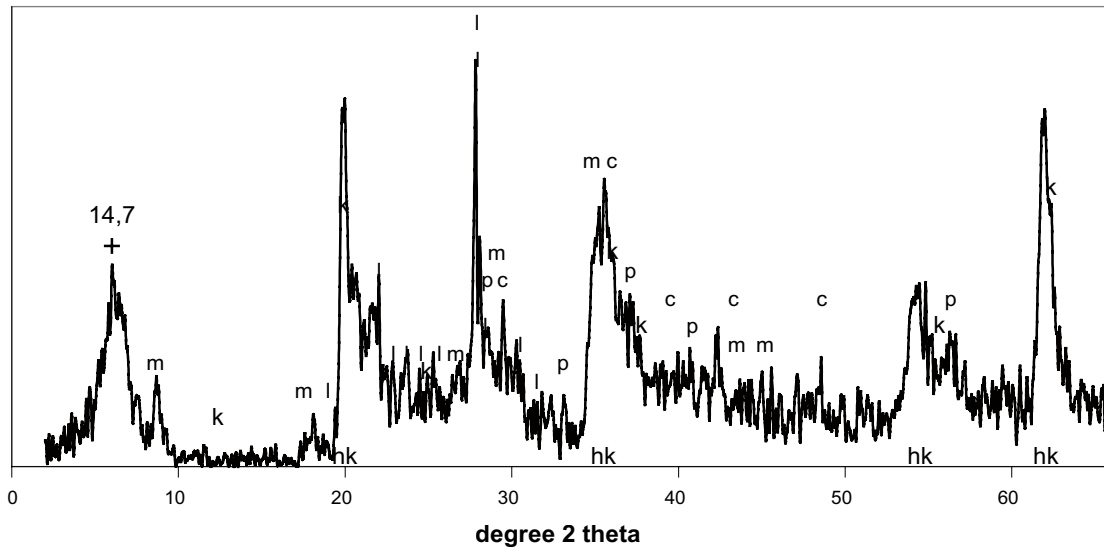


Figure 4-3. XRD-profile of random bulk sample of Milos BF 08. The position of the strongest peaks of the major non-clay minerals is indicated; l=Ca-plagioclase, c=calcite, k=kaolin mineral, m=mica/illite, p=pyrite. The centre of the (001) peak of the smectite at 14.7Å, the positions of the hk-bands and the (060)-peak are also indicated. CuK α radiation.

Table 4-7. Quantitative evaluation of the XRD data for the bulk of Milos BF 08 by use of the Siroquant software. The resulting chemical composition is given together with the results of the chemical analysis of the sample (ICP-AES and evolved-gas analysis) for comparison.

Siroquant Mineral phases	%	Normative mineral composition										
		Si %	Al %	Ti %	Fe %	Mg %	Ca %	Na %	K %	C %	S %	
Montmorillonite	70	20.19	7.82	0.27	2.89	1.46	1.04	0.43				
Mixed layer illite	3	0.77	0.43	0.01	0.13	0.04			0.23			
Illite	12	2.86	1.6	0.04	0.47	0.16			0.86			
Anatase	0.3			0.18								
Calcite	0.6						0.26			0.08		
Cristobalite	0.7	0.32										
Goethite	2.0				1.25							
Gypsum	0.7						0.17				0.13	
Kaolin	2.0	0.51	0.29				0.14	0.08				
Labradorite	6	1.62	0.93				0.46	0.26				
Pyrite	1.5				0.72						0.82	
Σ	99	26.27	11.07	0.5	5.46	1.66	2.07	0.77	1.09	0.08	0.95	
Oxides		SiO ₂	Al ₂ O ₃	TiO ₂	Fe ₂ O ₃	MgO	CaO	Na ₂ O	K ₂ O	Tot C	Tot S	Σ excl O/H
Σ		56.3	20.9	0.8	7.8	2.8	2.9	1.0	1.3	0.08	0.95	94.9
ICP-AES												
Milos BF 08		58.4	18.6	0.74	6.4	2.6	2.1	1.1	0.5	0.16	0.99	91.5

Kutch BF 04 and Kutch BF 08

Compared with the Milos samples, the iron content of the samples from Kutch is ca. three times higher and the samples also have higher concentrations of most of the other heavy metals, such as Ti, Cu, Zn, Ni, Co (Table 4-5), which reflects the difference in parent rock composition. Some of the source minerals of the heavy metals exist as discrete, crystalline phases – for instance anatase and rutile are the major Ti-bearing minerals and magnetite, goethite, and hematite/maghemite are the major Fe-bearing accessory minerals. Part of the CBD-extractable iron probably also exists as poorly crystalline, X-ray amorphous phases, which are not included in the Siroquant analysis or in the normative chemical composition.

Both Kutch samples are essentially carbonate-free. Kutch BF 04 contains some sulphate (0.11% S) probably derived from gypsum and peak positions for gypsum are indicated in the XRD-trace (Figure 4-4 and Table 4-8). However, according to the chemical data the maximum amount of gypsum that can exist (i.e. if all sulphur is allocated to $\text{CaSO}_4 \cdot 2\text{H}_2\text{O}$) is below 1%, which is close to the detection limit of the XRD analysis. Similarly, apatite is probably a major source of phosphorous in both samples, but again, the quantity is close to the detection limit of the XRD-method and the results of the Siroquant analysis must be considered uncertain at these low quantities.

The two samples have similar compositions with respect to accessory minerals, the only exception being quartz which is more abundant in Kutch BF 08. The quantitative evaluation also suggests that the smectite content is similar in both samples, approximately 80%. The differences between the two Kutch samples in the proportions of CaO and Na_2O are consistent with the composition of the pool of exchangeable cations – sodium alone saturates ca. 80% of the exchange sites in Kutch BF 08, whereas sodium together with calcium predominate the cation pool of Kutch BF 04 (cf. Table 4-3).

Basal spacings in the range 12.5–12.9 Å are typical of the monolayer hydrate of Na-smectites, which is stable at relative humidities below 60–70% /Brindley and Brown 1980/. Both samples from Kutch (Figure 4-3 and 4-4) have their (001) basal reflection centred around ca. 12.5 Å but the peaks are asymmetrical towards the low-angle side. Peak asymmetry or resolved first order peaks can generally be seen in mixed Na-Ca (Mg) smectite if conditions are such that the interlayers with divalent cations have two layers of water molecules and the Na-layers only one layer of water molecules.

Kutch BF 04 bulk

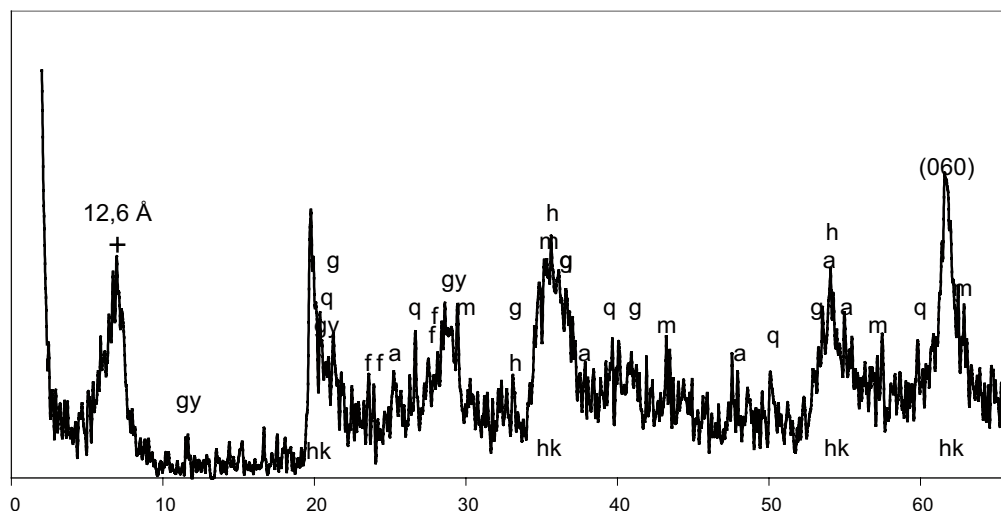


Figure 4-4. XRD-profile of random bulk sample Kutch BF 04. The position of the strongest peaks of the major accessory minerals is indicated, a=anatase, f=feldspars, g=goethite, gy=gypsum, h=hematite, m=maghemite/magnetite, q=quartz. The (001) peak of Na-smectite at 12.6Å, the positions of the hk-bands and the (060)-peak are also indicated. CuKα radiation.

Table 4-8. Quantitative evaluation of the XRD data for the bulk of Kutch BF 04 by use of the Siroquant software and the resulting chemical composition. The results of the chemical analysis of the sample (ICP-AES and evolved gas analysis) is included for comparison.

Siroquant Mineral phases	%	Normative mineral composition											%
		Si %	Al %	Ti %	Fe %	Mg %	Ca %	Na %	K %	P %	C %	S %	
Montmorillonite	78	22.19	7.63	0.34	4.45	1.71	0.53	1.05					
Anatase	1.7			1.00									
Apatite, hydroxy	1.2						0.47			0.22			
Calcite	2						0.79				0.24		
Goethite	3				2.01								
Gypsum	0.9						0.21					0.17	
Hematite	0.8				0.57								
Kaolin	2	0.37	0.35										
Labradorite	1.8	0.48	0.28				0.14	0.08					
Maghemite	2.1				1.49								
Magnetite	0.9				0.65								
Microcline	0.5	0.14	0.04						0.06				
Orthoclase	3	0.8	0.26						0.37				
Quartz	1.2	0.55											
Rutile	0.6			0.36									
Σ	99	24.53	8.56	1.71	9.17	1.71	2.14	1.13	0.43	0.22	0.24	0.17	
Oxides		SiO ₂	Al ₂ O ₃	TiO ₂	Fe ₂ O ₃	MgO	CaO	Na ₂ O	K ₂ O	P ₂ O ₅	Tot C	Tot S	Σ excl O/H
Σ		52.6	16.2	2.8	13.1	2.8	3.0	1.5	0.52	0.50	0.24	0.17	93.5
Kutch BF 04		51.1	14.9	2.9	16.2	3.3	2.0	1.9	0.06	0.29	0.21	0.11	92.8

Kutch BF 08

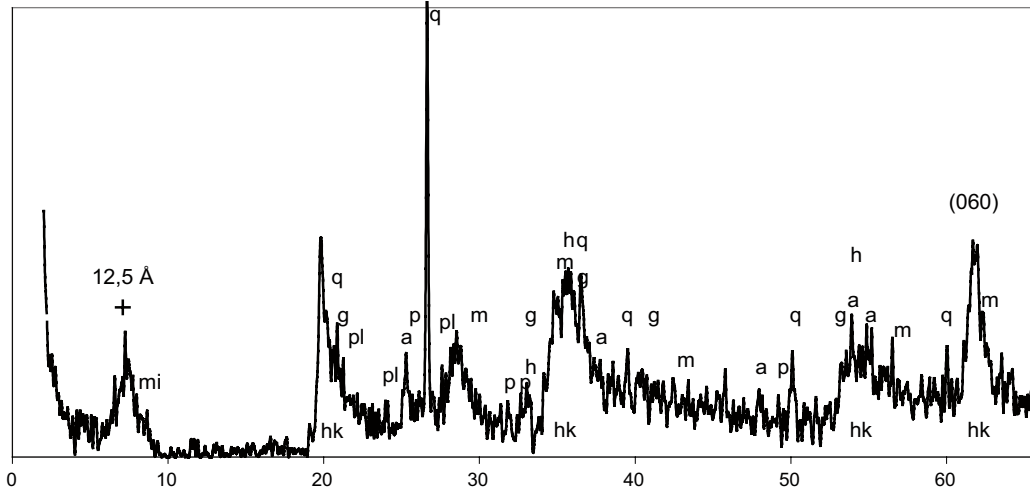


Figure 4-5. XRD-profile of random bulk sample Kutch BF 08. The position of the strongest peaks of the major accessory minerals is indicated; a=anatase, g=goethite, h=hematite, m=maghemite/magnetite, mi=mica/illite, p=apatite, pl=plagioclase, q=quartz. The (001) peak of Na-smectite at 12.2Å, the positions of the hk-bands and the (060)-peak are also indicated. CuKα radiation.

Table 4-9. Quantitative evaluation of the XRD data for the bulk of Kutch BF 08 by use of the Siroquant software and the resulting chemical composition. The result of the chemical analysis of the sample (ICP-AES and evolved-gas analysis) is included for comparison.

Siroquant Mineral phases	%	Normative mineral composition											
		Si %	Al %	Ti %	Fe %	Mg %	Ca %	Na %	K %	P %	C %	S %	
Montmorillonite	80	22.24	8.48	0.52	5.27	1.19	0.12	1.50					
Anatase	2			1.47									
Apatite, hydroxy	0.9						0.35			0.16			
Calcite	0.5						0.21				0.06		
Goethite	0.5				0.3								
Gypsum	0.7						0.17					0.13	
Hematite	1.1				0.74								
Kaolin	1.8	0.39	0.37										
Maghemite	1.5				1.1								
Magnetite	1.2				0.87								
Microcline	0.5	0.17	0.05						0.08				
Muscovite	2	0.44	0.42						0.21				
Quartz	6	2.62											
Σ	99	25.87	9.32	1.99	8.28	1.19	0.85	1.50	0.286	0.16	0.06	0.13	
Oxides		SiO ₂	Al ₂ O ₃	TiO ₂	Fe ₂ O ₃	MgO	CaO	Na ₂ O	K ₂ O	P ₂ O ₅	Tot C	Tot S	Σ excl O/H
Σ		55.4	17.6	3.3	11.8	2.0	1.2	2.0	0.34	0.37	0.06	0.13	94.3
ICP-AES													
Kutch BF 08		51.93	17.53	3.43	13.41	2.35	0.98	2.61	0.08	0.43	0.18	0.07	93.0

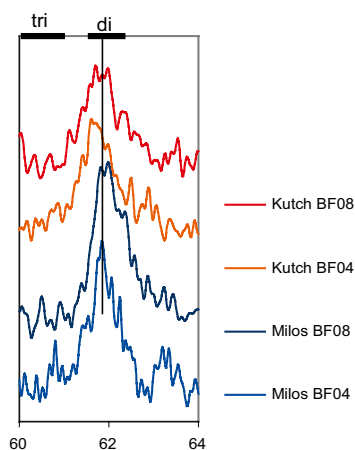


Figure 4-6. Close-up of the (060)-peak position. The *d*-values of the (060)-peak indicated by “*di*” ($1.49\text{--}1.50\text{ \AA} = 62.3\text{--}61.85^\circ 2\theta$) is typical of dioctahedral smectites. The position of the (060)-peak of trioctahedral smectites is also indicated. Cu *K* α radiation.

A close-up of the region $60\text{--}64^\circ 2\theta$ (i.e. scan resolution is not changed) of the XRD-profiles of all the samples (Figure 4-6) shows that the *d*-values of the (060) peaks range from 1.49 to 1.50 \AA , which is typical of the dioctahedral sub-group of smectites, to which montmorillonite, beidellite and nontronite belong. Thus, the available XRD-data provide no evidence of any significant difference in the *b* cell dimension of the smectite minerals, which would be an expected effect of, for instance, different cations or site occupancy in the octahedral sheet. However, both Milos samples, which appear to be free of quartz at the detection limit of the XRD method, have peaks of low intensity in the region $1.54\text{--}1.52\text{ \AA}$ (quartz has a peak of low intensity at 1.541 \AA) indicating that some trioctahedral phyllosilicate(s) may exist.

4.6 Chemical and mineralogical composition of the $<1\text{ }\mu\text{m}$ fraction of the bentonites

The chemical composition of the fraction $<1\text{ }\mu\text{m}$ is given in Table 4-10 for two sub-samples of each bentonite saturated with different index cations, Na and Sr. The data in Table 4-10 have been used for the calculations of the structural formula of the smectites presented in Table 4-13.

These calculations are based on the following assumptions and simplifications:

- The **iron** content of the $<1\text{ }\mu\text{m}$ fraction was corrected for CBD-extractable iron according to Table 4-11. Structural iron in the clay minerals was assumed to be trivalent although no determination was made of the oxidation state. The assumption that all octahedral iron is present only in the ferric state may underestimate the octahedral charge.
- All **potassium** was allocated to illitic layers in the smectite structure, since no discrete potassium-bearing minerals were detectable in any of the XRD-profiles of the $<1\text{ }\mu\text{m}$ fractions (Figure 4-7 and 4-8). The assumption was further justified by the values of the parameter $^\circ\Delta 2\theta$ (the difference in the 2θ position of the 002/003 and 001/002 reflections of illite/EG-smectite), which are given for all samples in Table 4-12. The $^\circ\Delta 2\theta$ values of the Kutch samples are indicative of almost pure smectite and the potassium content of these samples is very low (between 0.02 and 0.04% K_2O). In contrast, the $^\circ\Delta 2\theta$ values of the Milos samples suggest that the smectite structure may contain between 5 and 10% illitic layers, which would explain the higher potassium content of the Milos samples (1 and 0.4% K_2O , respectively). The proportion of illitic layers was calculated assuming their average K_2O -content to be 8.5% and the layer charge 1.5 per formula unit, which is intermediate between the extreme values reported for clay-sized micas/illites /Newman and Brown 1987/.
- Apart from I/S mixed layers in the Milos samples, all samples have been assumed to be pure smectite, although “contamination” of Milos 08 BF by traces of a kaolin mineral is indicated by peaks of low intensity at ca. 7 and 3.5 \AA in the diffraction profile of the $<1\text{ }\mu\text{m}$ fraction (Figure 4-7). No correction has been made for kaolinite in the formula calculation, and this fact necessarily adds to the sources of error in the structural formula of Milos BF 08.

Table 4-10. Chemical composition of the <1 µm fraction of the samples Milos BF 04, Milos BF 08, Kutch BF 04 and Kutch BF08. The samples have been saturated with Na and Sr, respectively, and dialysed prior to analysis. Major, minor and trace elements determined by ICP-AES, S and C by evolved gas analysis in a Leco furnace. n.d.=not determined.

Sample id.	SiO ₂ %	Al ₂ O ₃ %	Fe ₂ O ₃ %	MgO %	CaO %	Na ₂ O %	K ₂ O %	TiO ₂ %	P ₂ O ₅ %	MnO %	Cr ₂ O ₃ %	Sr ppm	(SrO) %	LOI %	Sum %	TOT/C %	TOT/S %
Milos BF04Na	53.02	17.84	5.07	3.34	0.31	1.84	1.03	0.97	0.03	0.01	0.009	180		16.4	99.90	0.56	<0.02
Milos BF04Sr	48.80	16.4	4.66	2.99	0.17	0.03	0.95	0.9	0.1	0.01	0.008	33,581	(3.99)	20.9	99.93	0.41	<0.02
Milos BF08Na	58.12	20.93	5.73	2.47	0.15	2.23	0.43	0.56	0.04	0.01	<0.002	134		9.2	99.91	0.31	<0.02
Milos BF08Sr	55.61	19.31	5.41	2.29	0.14	0.09	0.38	0.54	0.1	<0.01	<0.002	33,892	(4.01)	12.0	99.92	0.24	<0.02
KutchBF04Na	51.29	15.57	10.83	2.84	0.35	2.41	0.04	0.63	0.07	0.03	0.014	153		15.7	99.91	0.22	<0.02
KutchBF04Sr	47.08	14.3	9.95	2.57	0.26	0.06	0.02	0.58	0.17	0.03	0.013	39,016	(4.63)	20.2	99.94	0.19	<0.02
KutchBF08Na	51.95	17.56	10.52	1.99	0.44	2.24	0.02	0.95	0.02	0.03	0.016	43		14.1	99.96	0.15	<0.02
KutchBF08Sr	48.65	16.59	9.77	1.85	0.36	0.06	0.02	0.89	0.24	0.02	0.015	38,318	(4.54)	16.8	99.92	0.14	<0.02

Table 4-10 continued.

Sample id.	Cu ppm	Ba ppm	Zn ppm	Ni ppm	Co ppm	Zr ppm	Ce ppm	Y ppm	Nb ppm	Sc ppm	Ta ppm
Milos BF04Na	33	142	83	28	<20	179	54	9	8	14	<20
Milos BF04Sr	32	116	79	22	<20	167	49	10	5	12	<20
Milos BF08Na	n.d	40	n.d	<20	n.d	148	n.d	10	12	14	n.d
Milos BF08Sr	n.d	41	n.d	<20	n.d	143	n.d	10	8	14	n.d
KutchBF04Na	139	<5	91	66	<20	132	39	19	<5	37	<20
KutchBF04Sr	130	<5	80	52	<20	123	34	18	<5	33	<20
KutchBF08Na	196	<5	117	90	<20	123	51	25	10	43	<20
KutchBF08Sr	184	<5	108	89	<20	115	46	24	7	41	<20

Table 4-11. CBD-extractable iron (as oxide in weight % of the dry matter) of the Sr-saturated <1 μm fraction of the Milos and the Kutch samples. Total iron concentrations of the Sr-clays (from Table 4-10) are also given together with the CBD-extractable fraction.

Sample id	CBD-extractable Fe ₂ O ₃ %	Total Fe ₂ O ₃ %	CBD-extractable fraction
Milos BF04 <1μm	0.12	4.66	0.03
Milos BF08 <1μm	0.09	5.41	0.02
Kutch BF04 <1μm	1.87	9.95	0.19
Kutch BF08 <1μm	2.03	9.77	0.21

Table 4-12. The values of the parameter °Δ2θ (the difference of the position of the 002/003 and 001/002 reflections of illite/EG-smectite) of the Kutch and Milos samples. Comparison is made with the values for calculated diffraction profiles of I/S minerals with increasing proportions of illitic layers (from /Moore and Reynolds 1989/).

% illite	001/002		002/003		°Δ2θ
	d (Å)	°2θ	d (Å)	°2θ	
0	8.46	10.46	5.63	15.73	5.27
Kutch BF 04	8.51	10.40	5.63	15.73	5.33
Kutch BF 08	8.51	10.40	5.63	15.74	5.34
Milos BF 08	8.48	10.42	5.62	15.78	5.36
Milos BF 04	8.51	10.39	5.61	15.8	5.41
10	8.58	10.31	5.61	15.80	5.49
20	8.67	10.20	5.58	15.88	5.68
30	8.77	10.09	5.53	16.03	5.94
40	8.89	9.95	5.50	16.11	6.16

Another type of contamination that may be pertinent for the Milos bentonites in particular is the possible occurrence of non-crystalline, X-ray amorphous phases, such as free silica and remnant volcanic glass, which are known to exist in some of the bentonite deposits on Milos /e.g. Christidis and Dunham 1993, Christidis 1998/. “Contamination” of the smectite by, for instance, free silica would decrease the calculated tetrahedral charge and the total layer charge.

- Any **calcium** that may exist after the dialysis of the Na- or Sr-saturated clays was assigned to the pool of interlayer cations.
- The amount of octahedral **magnesium** was assumed to be equal in smectite samples extracted from the same bentonite but saturated with different index cations. An excess of Mg in the Na-saturated sub-sample of Milos BF 04 was therefore assigned to the pool of interlayer cations. Allocation of too much Mg to octahedral sites would underestimate the calculated amount of interlayer cations and this source of error is probably most important for the dolomite-rich Milos BF 04 in which release of Mg from any remnant carbonate during dialysis would lead to replacement of the interlayer index cation.

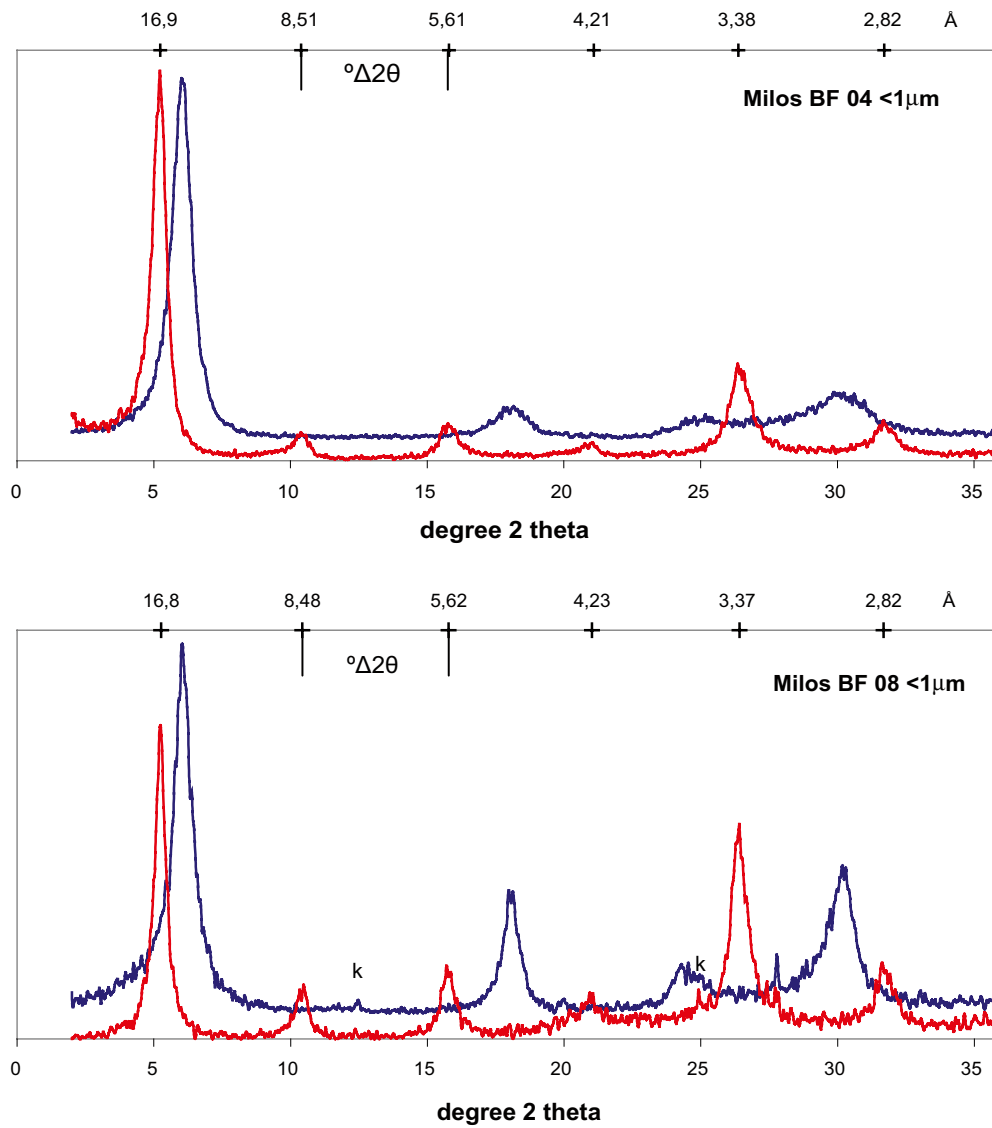


Figure 4-7. XRD-profiles of air-dried (blue) and EG-solvated (red) samples of <1 μm fraction of the Milos samples. k=kaolin mineral. The distance $^{\circ}\Delta 2\theta$ given in Table 4-12 is indicated.

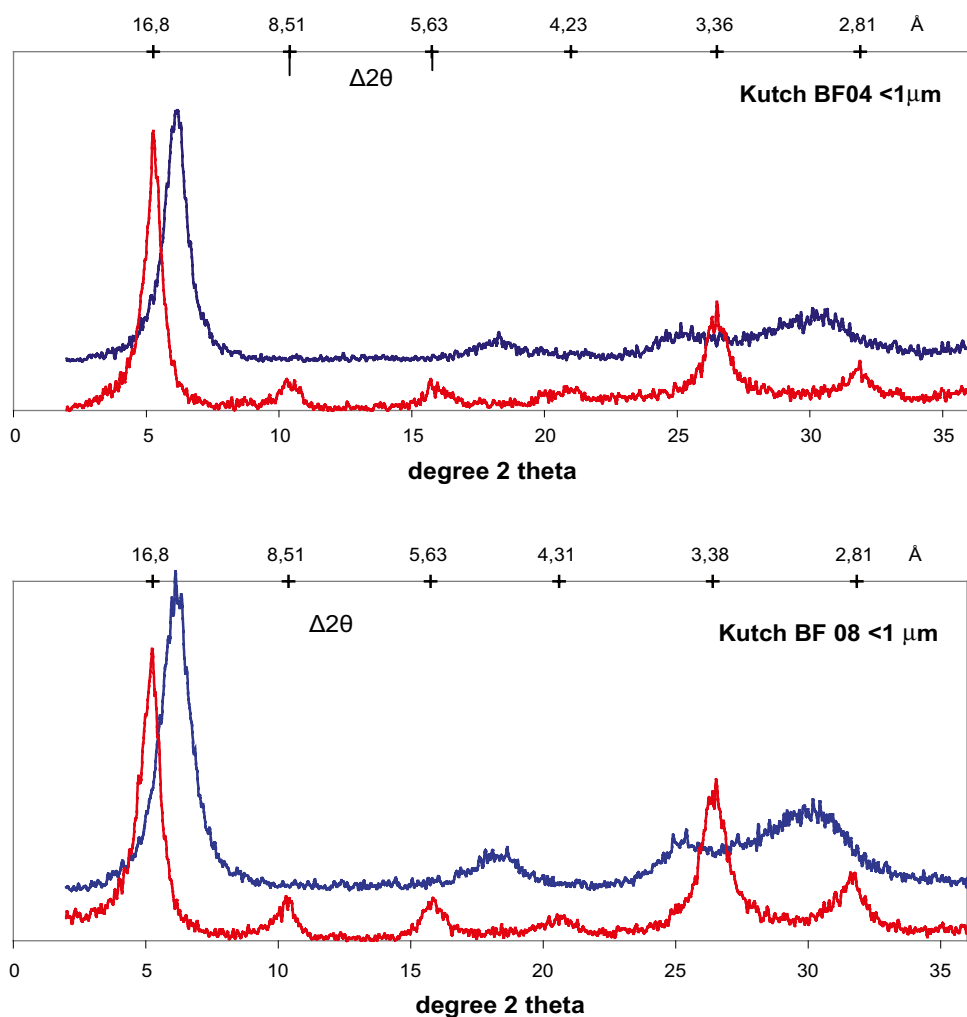


Figure 4-8. XRD-profiles of air-dried (blue) and EG-solvated (red) samples of <1 μm fraction of the Kutch samples. The distance $^{\circ}\Delta 2\theta$ given in Table 4-12 is indicated.

The calculated structural formulas are given in Table 4-13 together with the calculated and measured CEC of the <1 μm -fraction (Na-saturated). The results indicate that the <1 μm -fraction of the Kutch samples is almost pure smectite. The smectite in both Kutch bentonites is iron-rich with $\text{Fe} > \text{Mg}$ in the octahedral sheet. The structural formulas further suggest that a fairly high proportion of the charge is located in the tetrahedral sheet and, strictly, the smectite of Kutch BF 08 should be classified as beidellite rather than montmorillonite according to the charge distribution.

In contrast, the clay mineralogy of both Milos samples is more complex. The smectite of both samples is a montmorillonite which is interstratified with 5–10% illitic layers. In addition, the <1 μm fraction of Milos 08 BF contains traces of a kaolin mineral. Dilution of the smectite by clay minerals with low cation exchange capacity certainly reduces the CEC of <1 μm fraction but the fact that Milos BF 08 has the lowest CEC among the samples analysed is also due to the lower total layer charge of the smectite, around 0.70 p.f.u. compared to 0.80 p.f.u. or more for the other bentonite samples. The proportion of octahedral Mg is higher than octahedral Fe in the smectite of Milos BF 04, whereas Fe exceeds Mg in the octahedral sheet of the smectite of Milos BF 08.

Table 4-13. Calculated structural formula of the smectite in Milos BF 04, Milos BF 08, Kutch BF 04 and Kutch BF 08. Calculated CEC values (in meq/100 g) are given for the smectite and for the <1µm fraction, i.e. correction has been made for illitic layers, if present. *CEC of the <1µm fraction was measured for the Na-saturated sub-sample.

	Milos BF 04 Na	Milos BF 04 Sr	Milos BF 08 Na	Milos BF 08 Sr	Kutch BF 04 Na	Kutch BF 04 Sr	Kutch BF 08 Na	Kutch BF 08 Sr
Si	7.74	7.73	7.71	7.73	7.70	7.68	7.56	7.54
Al	0.26	0.27	0.29	0.27	0.30	0.32	0.44	0.46
Σ tet	8.0	8.0	8.0	8.0	8.0	8.0	8.0	8.0
Al	2.67	2.65	2.92	2.89	2.44	2.43	2.56	2.54
Ti	0.12	0.12	0.06	0.06	0.07	0.07	0.10	0.10
Fe3+	0.55	0.55	0.57	0.57	0.87	0.87	0.90	0.90
Mg	0.66	0.68	0.46	0.46	0.63	0.62	0.43	0.43
Σ oct	4.00	4.00	4.00	3.98	4.01	3.99	4.00	3.97
Ca	0.05	0.01	0.02	0.02	0.06	0.01	0.08	0.03
Mg	0.05	0.01	0.02	0.00	0.00	0.00	0.00	0.00
Na	0.58	0.01	0.60	0.03	0.70	0.00	0.63	0.00
Sr	0.00	0.41	0.00	0.34	0.00	0.43	0.00	0.41
interlayer charge	0.80	0.84	0.68	0.73	0.82	0.89	0.79	0.87
% tet. charge	33	32	43	37	37	36	56	53
% illitic layers	~11	~11	~5	~5	~0	~0	~0	~0
CEC smectite	106	109	90	95	108	114	101	112
CEC <1µm	95	97	85	91	108	114	101	112
CEC <1 µm measured*	103	103	89	89	112	112	106	106

5 Summary

Milos BF 04 is distinguished by a high content of carbonate minerals, dolomite and calcite, which make up almost 25% of the bulk sample. The content of sulphur-bearing minerals is very low (0.06% total S) and K-feldspars are the second most abundant non-clay mineral. Smectite makes up around 60% of the bulk sample. The smectite should be classified as montmorillonite with ca. 10% illitic layers and with octahedral Mg > octahedral Fe. CEC of the bulk sample is 73 meq/100 g and the pool of interlayer cations has a composition Mg>Ca>Na.

Milos BF 08 is low in carbonates but has the highest content of sulphur-bearing minerals (0.99% S) of the bentonites examined. There are strong indications that the major part of sulphur occurs as pyrite. Other accessory minerals of significance are Ca-rich plagioclase, kaolin mineral and mica/illite. The smectite content in the bulk sample is around 70%. The smectite should be classified as a montmorillonite with a few percent illitic layers and with octahedral Fe > octahedral Mg. The structural formula of the smectite suggests that the total layer charge is lower than that of the other samples examined. CEC of the bulk sample is 71 meq/100 g and the pool of interlayer cations has a composition Ca>Na>Mg.

Kutch BF 04 is low in both sulphur-bearing minerals and carbonates but has a high content of titanium- and iron-rich accessory minerals, such as anatase, magnetite, hematite and goethite. Other accessory minerals of significance are feldspars and quartz. The smectite makes up ca. 80% of the bulk sample and is a montmorillonite with octahedral Fe>octahedral Mg. CEC of the bulk sample is 97 meq/100 g and the pool of interlayer cations has a composition Na>Ca>Mg.

Kutch BF 08 is low in both sulphur-bearing minerals and carbonates. Also this sample has a high content of Ti- and Fe-rich accessory minerals of the same type as Kutch BF 04 and a similar suite of other accessory minerals. The smectite makes up ca. 80% of the bulk sample and is iron-rich with octahedral Fe>>octahedral Mg. Based on the charge distribution the smectite should be classified as beidellite. CEC of the bulk sample is 89 meq/100 g and the pool of interlayer cations has a composition Na>>Ca=Mg.

6 References

- Ammann L, Bergaya F, Lagaly G, 2005.** Determination of the cation exchange capacity of clays with copper complexes revisited. *Clay Minerals* 40. 441-453.
- Belyayeva N I, 1967.** Rapid method for the simultaneous determination of the exchange capacity and content of exchangeable cations in solonchic soils. *Soviet Soil Science*. 1409-1413.
- Brindley G W, Brown G, 1980.** Crystal Structures of Clay Minerals and their X-ray Identification. Mineralogical Society Mon. No. 5. 495 p.
- Christidis G, Dunham A C, 1993.** Compositional variation in smectites: Part I. Alteration of intermediate volcanic rocks. A case study from Milos Island, Greece. *Clay Minerals* 28, 255-273.
- Christidis G, 1998.** Comparative study of the mobility of major and trace elements during alteration of an andesite and a rhyolite to bentonite, in the islands of Milos and Kimolos, Aegean, Greece. *Clays and Clay minerals* 46. 379-399.
- Jackson M L, 1975.** Soil chemical analysis – advanced course. Second edition. Madison, Wisconsin, 991 p.
- Meier L P, Kahr G, 1999.** Determination of the cation exchange capacity (CEC) of clay minerals using the complexes of copper(II) ion with triethylenetetramine and tetraethylenepentamine. *Clays and Clay Minerals* 47, 386-388.
- Mehra O P, Jackson M L, 1960.** Iron oxide removal from soils and clays by a dithionite-citrate system buffered with sodium bicarbonate. *Clays and Clay Minerals* 7th National Conference. Pergamon Press. 317-327.
- Moore D M, Reynolds R C, 1989.** X-ray Diffraction and the Identification and Analysis of Clay Minerals. Oxford University Press. 332 p.
- Newman A C D, Brown G, 1987.** The Chemical Constitution of Clays. In Newman, A.C.D. (ed): *Chemistry of Clays and Clay Minerals*. Mineralogical Society Mon. No. 6. 1-128.
- Poppe L J, Paskevich V F, Hathaway J C, Blackwood D S, 2001.** Separation of the silt and clay fractions for X-ray powder diffraction by centrifugation. In: *A laboratory manual for X-ray powder diffraction*. US Geological Survey Open File Report 01-041
- Rietveld H M, 1969.** A profile refinement method for nuclear and magnetic structures. *J. Appl. Cryst.* 2. 65-71.
- Shah N R, 1997.** Indian bentonite – focus on the Kutch region. *Industrial Minerals* 359. 43-47.
- Taylor J C, Matulis C E, 1994.** A new method for Rietveld clay analyses. Part I. Use of a universal measured standard profile for Rietveld quantification of montmorillonite. *Powder Diffraction* 9. 119-123.